ACS OMEGA

http://pubs.acs.org/journal/acsodf

Article

Exploring the Phytochemical Profile and Biological Activities of *Clerodendrum infortunatum*

Balakrishnan Syamala Akhil,[⊥] Rajimol Puthenpurackal Ravi,[⊥] Asha Lekshmi, Prathapan Abeesh, Chandrasekharan Guruvayoorappan, Kokkuvayil Vasu Radhakrishnan,* and Kunjuraman Sujathan*

Cite This: *ACS Omega* 2023, 8, 10383−10396

Read Online

ACCESS | Metrics & More | Article Recommendations | Supporting Information

ABSTRACT: *Clerodendrum infortunatum* (*C. infortunatum*), the hill glory bower, is reputed as the prodigious treasure for Indian folk medicine. The study has focused on exploring the phytochemistry and antitumor potential of the *C. infortunatum* root extract *in vitro* and *in vivo*. The ethyl acetate root extract has demonstrated the highest cytotoxicity in a series of nine human tumor cell lines. Further fractionation of the same has yielded seven compounds. The structures of these compounds were confirmed with spectroscopic techniques. Considering the toxicity observed with the crude extract, cytotoxicity of these compounds was further assessed in two breast carcinoma cell lines (MCF-7[ER/PR-positive HER2-negative] and MDA-MB-231 [ER/PR/HER2-negative]) and in two cervical cancer [human papilloma virus (HPV)-negative C33A and HPV-positive SiHa] cell lines. Betulinic acid (BA) was found as the active principle contributing the cytotoxic activity, and cervical cancer cell lines documented the minimum IC_{50} value in 24 h. In order to validate the *in vitro* experimental data, we have established a xenograft model of HPV-positive cervical cancer in female NOD/SCID mice treated with BA using doxorubicin as the positive control. BA treatment gradually reduced the tumor size, maintaining healthy hematological and biochemical parameters, and improved the survival rate of tumor-bearing mice considerably. Thus, our findings suggest that the *C. infortunatum* root extract has a promising anticancer property against HPV-positive cervical cancer and supports its usage by traditional healers for treating cervical cancer.

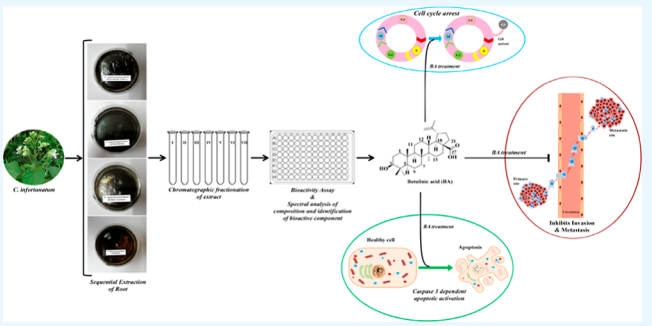

INTRODUCTION

Plants have been used for medicinal purposes in their raw form and in different formulations since ancient times. Folk medicine and Ayurveda practitioners depend on plant-based preparations to cure several diseases. As plant-derived medicines are relatively less toxic to normal cells and are better tolerated, there is a wide acceptance to drug development schemes based on Ayurvedic concepts. Several phytochemicals and their derived metabolites perform an array of pharmacological functions in the human system. Alkaloids, flavonoids, phenolics, tannins, glycosides, gums, resins, and oils are such responsible elements.[1] *Clerodendrum infortunatum* is one of the most studied plants among the 580 species of the family Verbenaceae considering its ease of availability, apparent beneficial properties of the plant parts, and the extensive use of it by traditional healers for treating several diseases including cancer.[2−4] The anti-cancer property of the alcoholic and aqueous extract of the root and leaf of the plant has been reported by several groups without characterizing the phytochemicals responsible for this activity. Only a few reports have documented the active components, each demonstrating the cytotoxicity in one or two cell lines.[5,6] The active component responsible for the cytotoxic effect has been reported to vary from glycoproteins[7] to abietane-type diterpenoidglycosides,[6] oleanolic acid, clerodinin A,[8] and so forth in these reports. Hence, a consensus could not be obtained, and none of these reports has been substantiated further, which prompted us to study the leaf and root extract in a systematic way to identify the potential cytotoxicity in a wide panel of human tumor cells with different characters and origins. Contradictory to many of the previous reports, betulinic acid (BA) was found to be responsible for the cytotoxic effect of the root extract, which has been chemically characterized and experimentally validated as a strong inhibitor of sustained proliferative signals and replicative immortality, the two major hallmarks of carcinogenesis. To the best of our knowledge, this study is the pioneer one among the available ambiguous reports, boosting up the prospective of BA extracted from *C. infortunatum* root for a clinical trial to

Received: December 20, 2022
Accepted: January 24, 2023
Published: March 6, 2023

© 2023 The Authors. Published by American Chemical Society

broach it as a potential commercial drug for human papilloma virus (HPV)-associated malignancies.

RESULTS AND DISCUSSION

The dried roots of *C. infortunatum* after pulverization were subjected to sequential extraction using the Soxhlet apparatus, and the extract obtained has been subjected to cytotoxicity assay. Sequential extraction of the powdered roots of *C. infortunatum* with different solvents yielded four extracts: petroleum ether extract (PE), chloroform extract (CL), ethyl acetate extract (EA), and methanol extract (ME). The antiproliferative potential of these extracts using MTT assay in an array of nine cell lines of diverse origin such as K562, A549, A375, HCT116, HepG2, MCF-7, MDA-MB-231, C33A, and SiHa in varying concentrations revealed that the toxicity varies depending on the cell type, solvent type, concentration, and time (Table 1). Unlike the previous reports of the hexane and chloroform root extract exhibiting significant toxicity against PC-3 (prostate), A549 (lung), T47D (breast), and HCT-116 (colon) cancer cell lines,[9] the EA root extract was found to have a maximum growth inhibition with respect to incubation time in all of the tumor cells studied. Breast cancer (MCF-7 and MDA-MB-231) and cervical cancer (C33A and SiHa) cell lines showed maximum cytotoxicity with HPV-positive cervical cancer cell lines (SiHa), recording the minimum IC_{50} value (203 μg/mL) after 24 h of treatment (Figure 1a,b).

Table 1. Cytotoxicity Effect of the Ethyl Acetate Root Extract of *C. infortunatum* Against Nine Tumor Cell Lines in Terms of Their IC_{50} Values

	C. infortunatum root (EA extract)	
cell lines	IC_{50} value (μg/mL) at 24 h	IC_{50} value (μg/mL) at 48 h
K562	463.41 ± 11.01	384.31 ± 10.01
A549	566.82 ± 07.04	619.51 ± 05.64
A375	450.31 ± 11.13	397.46 ± 06.43
HCT116	663.41 ± 10.15	650.73 ± 11.67
HepG2	351.22 ± 09.63	382.43 ± 05.36
MCF-7	338.26 ± 05.59	325.58 ± 06.55
MDA-MB-231	301.46 ± 05.82	343.41 ± 06.27
C33A	315.01 ± 03.86	304.44 ± 04.80
SiHa	203.90 ± 05.76	207.80 ± 03.30

With the phytochemical constituents being secondary metabolites of the plant, some inherent adverse effects on normal cells need to be ruled out. Varalakshmi et al. have shown that the leaf extracts of *Coleus aromaticus*, *Phyllanthus niruri*, and *Azadirachta indica* and the dried fruit rind of *Garcinia indica* potential anti-cancer agents are toxic to human peripheral lymphocytes at higher concentrations.[10] Therefore, the effect of the *C. infortunatum* root extract on normal peripheral lymphocytes was evaluated by lymphocyte proliferation assay. Figure 1c shows the rate of lymphocyte viability with respect to concentration of the extract. At the concentration ranging from 100 to 800 μg/mL, PE, CL, EA, and ME showed viabilities of 99−94%, 99−98%, 99−98%, and 98−97%, respectively. No significant toxicity was found after 72 h treatment with different concentrations (Figure 1c). Thus, it was confirmed that the *C. infortunatum* root extract is non-toxic to normal cells.

Fractionation Strategy of Root Extracts Using Silica Gel Column Chromatography. The *C. infortunatum*-EA root extract was further fractionated using silica gel column chromatography with the hexane EA solvent system to decipher its biochemical composition. Column chromatography and crystallization of fraction 1 (Fr. 1) yielded white needle-like crystals (19 mg) which were separated from the mother liquor and were named compound **1** and identified as β-sitosterol by comparing with previous literature reports.[11] Fraction pool Fr. 2 obtained was chromatographed again over the silica gel column using 15% EA−hexane polarity, yielding 16 mg of a colorless solid, compound **2**, which was then identified as stigmasterol by comparing the nuclear magnetic resonance (NMR) with the earlier reports.[12] Fraction pool Fr. 3 on column chromatography yielded 56 mg of compound **3** while eluting the column with 30% EA−hexane polarity, which was then identified as BA by comparing with previous reports.[13] Fraction pool Fr. 4 upon purification yielded 42 mg of compound **4** as a bright yellow solid; comparing the spectral data with the literature,[14] the structure of compound **4** was identified as retusin. Compound **5** was obtained by eluting the column with 60% EA−hexane, and the structure of the compound was confirmed to be oleanolic acid by spectral data comparison.[15] One more UV-active compound was isolated from the fifth fraction pool. This upon purification yielded 29 mg of compound **6**. By comparing these spectral data,[16] the structure of compound **6** was identified as ayanin. Another yellow solid was isolated next to ayanin by eluting the column of Fr. 6 with 70% EA−hexane polarity, counted as compound **7** (110 mg). The compound was confirmed as quercetin.[17]

Based on a comparison with the literature, we have successfully isolated seven compounds which were identified as β-sitosterol (**1**), stigmasterol (**2**), BA (**3**), retusin (**4**), oleanolic acid (**5**), ayanin (**6**), and quercetin (**7**). Figure 2 shows the structural formulae of these isolated molecules. Several other plants have been reported to possess BA as a secondary metabolite.[18,19] Many of these compounds were well discussed by researchers in various aspects of oncology.

The cytotoxicity of the aforementioned compounds was studied in breast and cervical cancer cell lines which were found to be most affected by this extract. The cell lines were treated with 25, 50, 100, and 200 μg/mL of each of the seven compounds, and MTT assay was carried out at 24 and 48 h. Compound **3**, BA, exhibited maximum cytotoxicity compared to all the other compounds (Figure 3). SiHa, HPV-positive cervical cancer cells, was found to be more sensitive (lower IC_{50} value: 37.65 μg/mL in 24 h) to BA (Table 2) compared to the other three cell lines, MCF-7 (IC_{50} = 125.26 ± 3.83 and 100.63 ± 7.02), MDA-MB-231 (IC_{50} = 137.95 ± 3.98 and 111.62 ± 7.51), and C33A (IC_{50} = 112.78 ± 7.14 and 83.72 ± 5.51) in 24 and 48 h respectively. BA is a pentacyclic triterpenoid already renowned for having cytotoxic properties against a number of human tumors as evident from studies in xenograft mouse models and primary tumor samples.[20] Kessler et al. have reported that a number of cells of diverse origin from lung, colorectal, breast, prostate, and cervix cancer are sensitive to BA treatment.[21] Previously, it has been proved that the anti-proliferative influence of BA in leukemia cells (U937) found that BA reduced cell viability through control cell cycle progression and apoptosis.[22] From our data, BA fractionated from *C. infortunatum*-EA was found to be active against the HPV-positive cervical cancer cell line.

BA Augments Apoptosis. As the cytotoxicity of BA was established, the apoptotic potential of BA was analyzed by dual live−dead staining using acridine orange and ethidium bromide to decipher the exact mechanism of action of BA

https://doi.org/10.1021/acsomega.2c08080
ACS Omega 2023, 8, 10383−10396

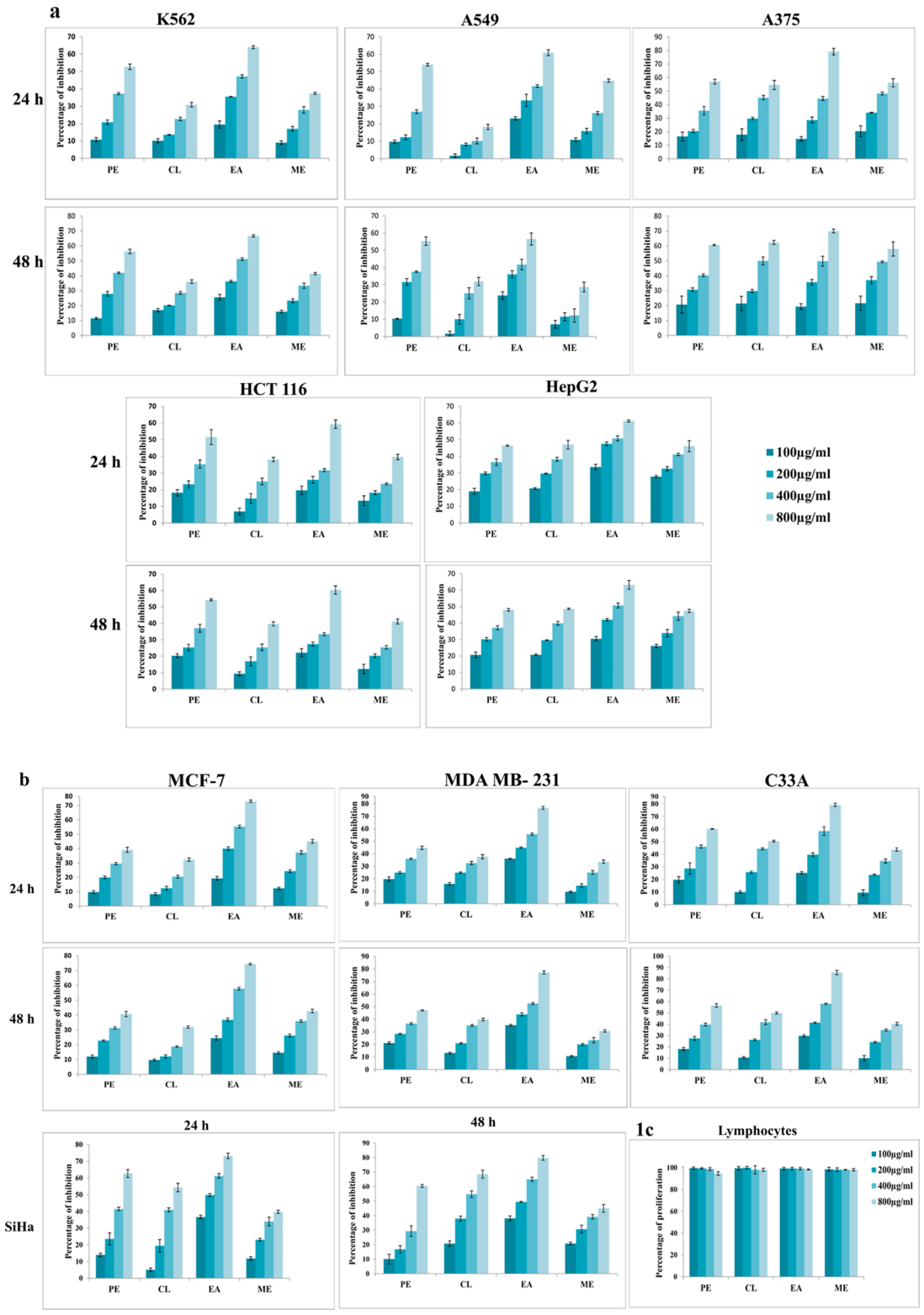

Figure 1. Cytotoxicity effect of the root extract of *C. infortunatum* from different solvents (PE, CL, EA, and ME) with increasing concentration (100, 200, 400, and 800 μg/mL) over different tumor cell lines (K562, A549, A375, HCT 116, HepG2, MCF-7, MDA-MB-231, C33A, and SiHa) using MTT assay at 24 and 48 h of incubation (a,b) and cell viability assay of human lymphocyte cells using the root extracts of *C. infortunatum* for 72 h of incubation (c).

on tumor cells. Uniform green fluorescence from the control cell nuclei indicated the lack of significant apoptosis, whereas granular yellow−green fluorescence of the BA-treated cells indicated the activation of the apoptotic cascade (Figure 4a). The DOX-treated cells showed both yellow and red fluorescence, indicating apoptotic and necrotic changes (Figure 4a). From this, it was hinted that BA activates apoptotic signaling in cancer cells.

https://doi.org/10.1021/acsomega.2c08080
ACS Omega 2023, 8, 10383−10396

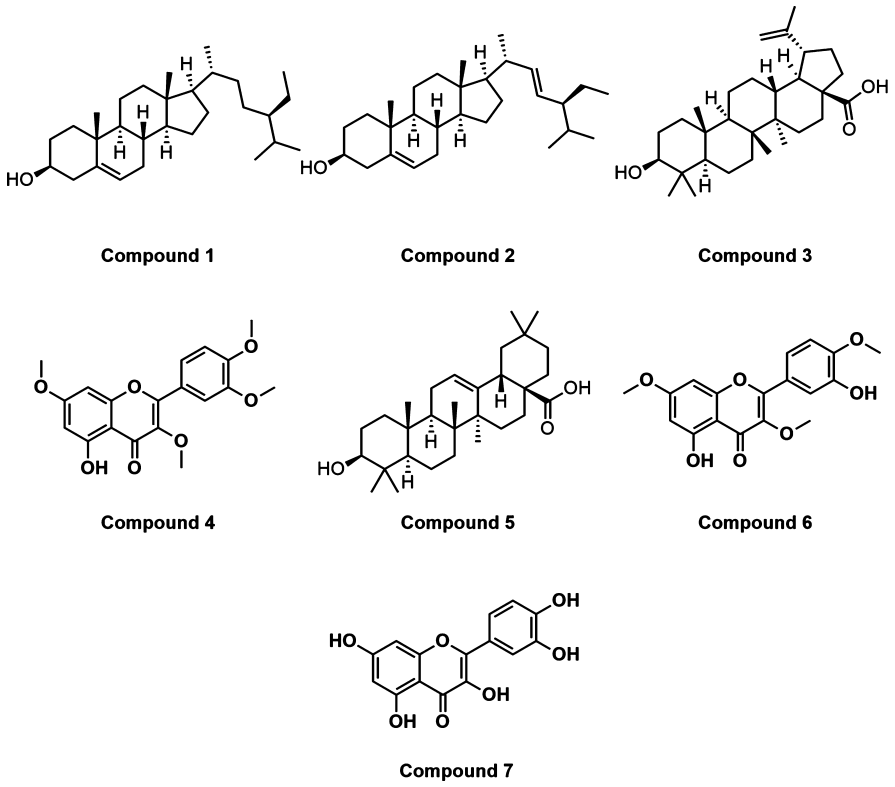

Figure 2. β-sitosterol (1), stigmasterol (2), BA (3), retusin (4), oleanolic acid (5), ayanin (6), and quercetin (7).

The apoptotic potential of BA was further validated by Hoechst staining and analysis of nuclear condensation. The untreated control cells appeared light blue in color with a round to oval nuclei and intact chromatin, whereas both BA- and DOX-treated cells showed much brighter fluorescence than the control cells with chromatin condensation and nuclear fragmentation (Figure 4b). A similar type of apoptotic sensitivity for nanoencapsulated BA treatment has already been reported in human colorectal cancer cells (HT-29).[23]

BA-mediated apoptosis in SiHa cells was further deliberated using annexin V/PI flow-cytometric analysis (Figure 5). Upon treatment with IC_{50} concentration of BA (37.6 μg/mL), SiHa cells shifted 62% of the cells to the early apoptotic quadrant and 5.36% of the cells to the late apoptotic one. These results further corroborated that BA has the potential to induce apoptosis in SiHa cells. Fulda (2008) has highlighted the mitochondrial (intrinsic) pathway-mediated apoptotic execution by BA.[24]

Through further study on the apoptotic pathway activated by BA, it was found that cell death is triggered in a caspase-3-dependent intrinsic pathway (Figure 7). Caspase activity was found in up to 52.27 ± 1.19 percent of cells. This went in hand with many recent reports, implying that BA may play a major role in the caspase-dependent apoptotic process in neuroectodermal[25] and hepatocellular carcinoma.[26,27] It is also reported that BA has the capacity to inhibit antiapoptotic proteins and can upsurge proapoptotic protein levels. Mitochondria release cytochrome C and increase the levels of caspase-3 and caspase-9 results in cell apoptosis.[28]

The cell cycle analysis using FACS revealed a significant increase in the percentage of G_0 fraction upon BA treatment (Figure 6), indicating the crucial role of BA in impeding growth signal self-sufficiency, a vital characteristic attribute of tumor cells. The significance of BA in inhibiting the replicative potential has already been discussed. BA disturbs cell cycling by promoting the degradation of cell cycle-related protein cyclins A, B1, and D1; kinases such as Cdk1, 2, and 4, and transcription factor E2F1. Similar to camptothecin, BA directly interacts with mammalian type I DNA topoisomerase, preventing the formation of a binary complex with DNA there by deterring its catalytic activity.[29]

BA Inhibits Tumor Metastasis and Invasion. BA was found to inhibit growth and proliferation and activate cell death in cancer cells. Hence, it was thought of delving into its effect on other oncogenic parameters such as tumor invasion and migration. Transwell chamber assay showed a significantly suppressed migration potential of SiHa cells following BA treatment (Figure 8a,b), and the number of migrating cells was 177 ± 6.16 (BA), 117 ± 3.85 (DOX), and 549 ± 15.36 (control). Similarly, in the invasion assay, untreated SiHa cells were found to move freely in the Matrigel toward the lower chamber of the Transwell plate, indicating that BA treatment effectively suppresses the invasion potential of SiHa cells (Figure 8c,d) in the same way as DOX does. The number of invaded cells in the untreated membrane was 622 ± 10.98 and BA-treated membrane was 164.33 ± 4.64 followed by 122.66 ± 3.85 cells in the DOX (positive control)-treated chamber.

The potential of BA to inhibit cell migration was further reinforced by wound healing assay (Figure 8e,f). It has been reported that BA decreases migration and invasion abilities in bladder cancer cells (T-24, UMUC-3, and 5637) and in breast cancer cells (MDA-MB-231 and BT-549).[30] Here, the control cells reached confluency on the "wound" created over a period of 48 h, while the BA treatment impedes the tumor cells (SiHa) from wound closure with substantial inhibition in migration rate.

***In Vivo* Validation of the Cytotoxic Effect of BA.** The antitumor activity of BA on cervical cancer was evaluated *in*

https://doi.org/10.1021/acsomega.2c08080
ACS Omega 2023, 8, 10383−10396

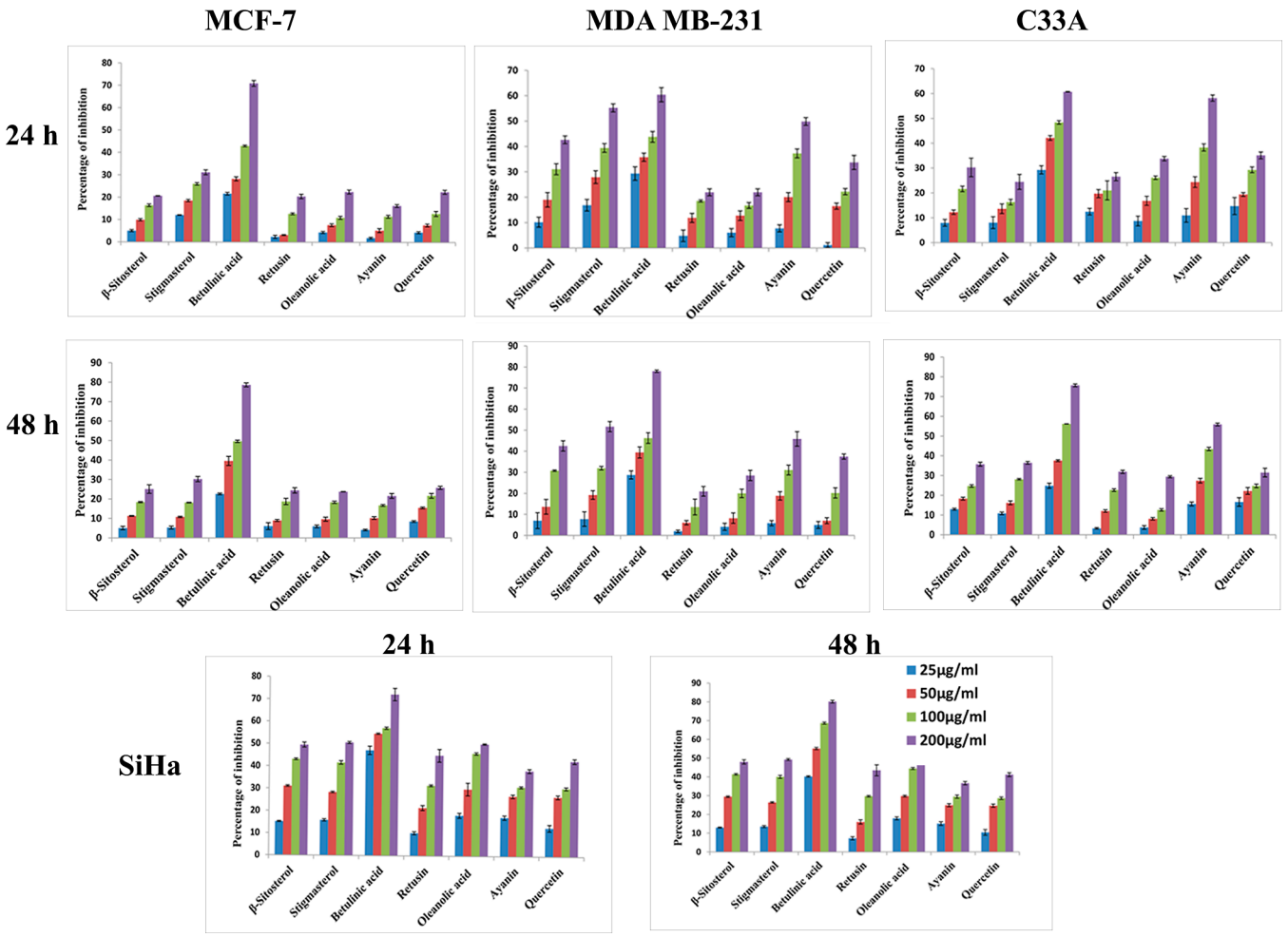

Figure 3. Cytotoxicity effect of seven compounds (*β*-sitosterol, stigmasterol, BA, retusin, oleanolic acid, ayanin, and quercetin) isolated from *C. infortunatum*-EA on MCF-7, MDA-MB-231, C33A, and SiHa over 24 and 48 h using MTT assay.

Table 2. Cytotoxicity Effect of BA in 24 and 48 h against Two Breast Cancer and Cervical Cancer Cell Lines

	BA	
cell Lines	IC_{50} value (*μ*g/mL) at 24 h	IC_{50} value (*μ*g/mL) at 48 h
MCF 7	125.26 ± 3.83	100.63 ± 7.02
MDA-MB-231	137.95 ± 3.98	111.62 ± 7.51
C33A	112.78 ± 7.14	83.72 ± 5.51
SiHa	37.65 ± 2.65	41.86 ± 3.06

vivo in NOD/SCID mice. Cervical cancer xenografts were developed in the left lower flank of each mouse by subcutaneous injection of SiHa cells, and tumor growth was monitored. BA was administered intraperitoneally, and its effect was evaluated in tumor growth.

Representative images of tumor-bearing animals and resected tumors (day 30) from each group are shown in Figure 10. A reduction in tumor volume and tumor size and enhancement of lifespan were observed in animals treated with BA and DOX (Figure 10c,e). Mice group treated with BA (tumor + BA) showed the highest increase in life span (more than 65 days) (log rank test p value < 0.001) compared to the tumor-bearing control group and positive control (DOX). Reduction in tumor burden and enhancement of survival are often regarded as the most significant features of an anti-tumor experimental drug.[31−34] Treatment with BA was found to resist the aggravation of the cervical cancer xenograft (induced tumor burden) in NOD/SCID mice as evidenced by the reduction in tumor load. Figure 10b shows neovascularization found around the tumor xenograft in the inner peritoneal lining of tumor-bearing animals. A marked reduction in the sprouting of new blood vessels was observed in xenograft-bearing mice treated with BA and DOX (positive control), compared to the tumor control.[35] The molecules which inhibit the tumor directed sprouting of new blood vessels has been considered as potential anti-cancer agents which could inhibit the metastatic cascade.[36] In our study, BA has been showen to inhibit tumor specific neovascularization thereby exhibiting tumor cell invasion and metastasis which might be the possible reason for its cancer therapeutic effect.

Figure 10f shows the histopathologic features of tumor dissected from NOD/SCID mice. Densely packed highly proliferating round to oval cells with hyperchromatic nuclei and a high nuclear cytoplasmic ratio were observed, whereas the BA-treated tissue section showed loosely arranged scattered tumor cells with degenerative changes like nuclear condensation, nuclear fragmentation, cytoplasmic vacuolation, cytoplasmic eosinophilia, and evidence of tumor clearance (Figure 10f). Areas of marked necrosis were also observed.

Evaluation of the Toxicity of BA. The hematological and biochemical profile of the experimental animals were analyzed. Figure 9 shows the hemoglobin (Hb) content and complete

https://doi.org/10.1021/acsomega.2c08080
ACS Omega 2023, 8, 10383−10396

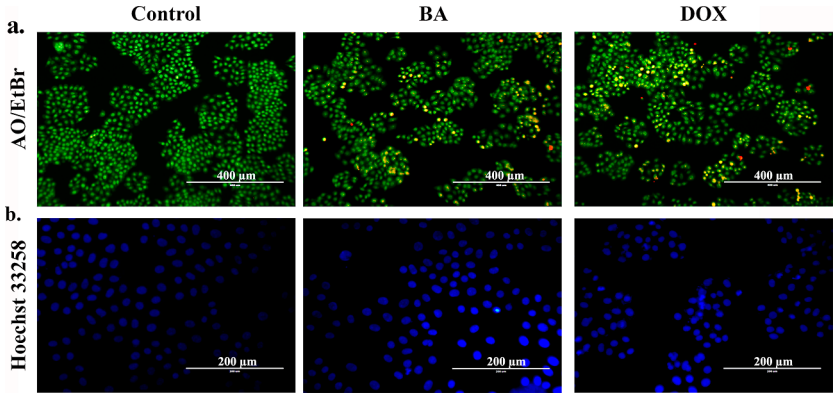

Figure 4. Morphological evaluation of apoptosis in SiHa cells treated with BA and DOX for 24 h of incubation using acridine orange/ethidium bromide dual staining (a) and Hoechst staining (b).

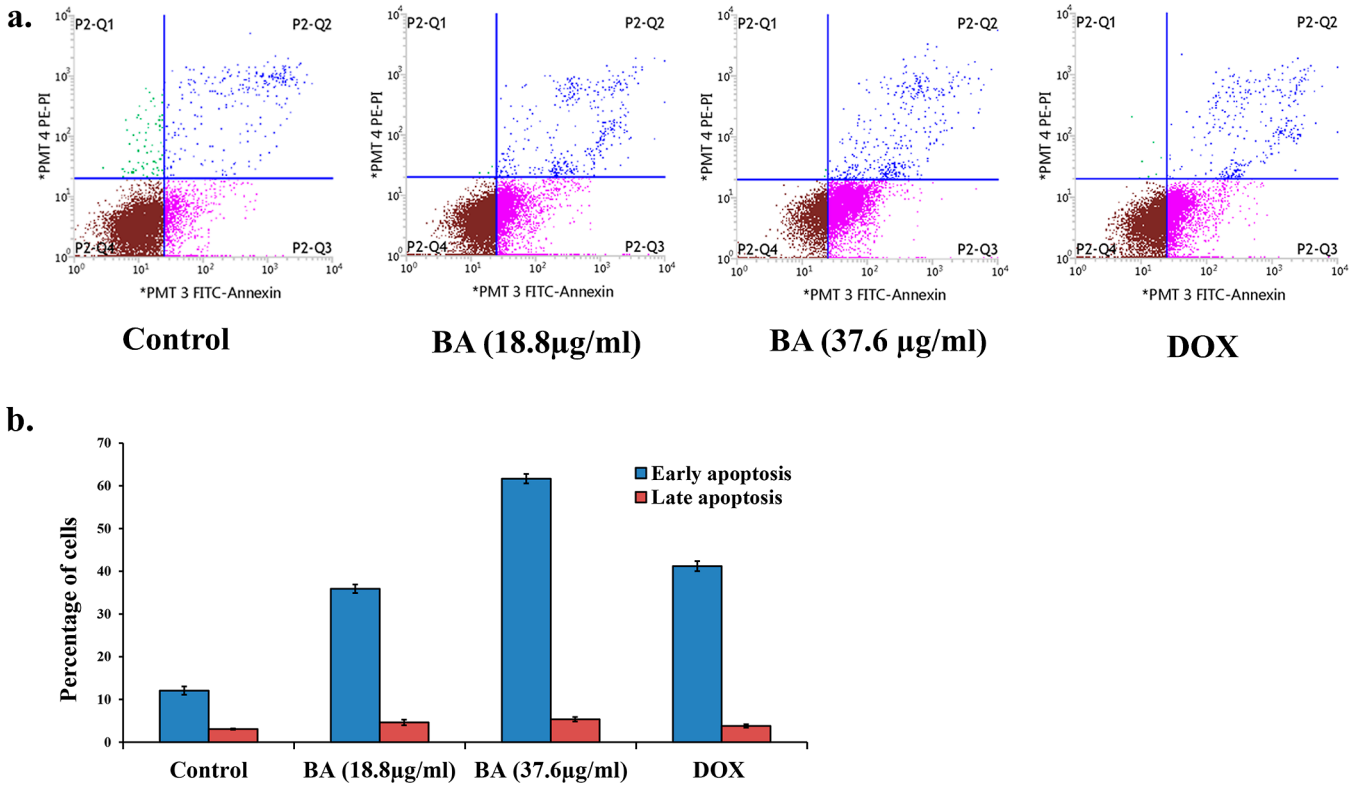

Figure 5. Annexin V/PI flow cytometric analysis of control and treated (BA and DOX) SiHa cells for 24 h of incubation. (a) Scatter plot (b) and graphical representation of early and late apoptotic cells after the treatment. Data were expressed as mean ± SD from triplicate experiments.

blood count of blood collected from the mice by cardiac puncture. SiHa tumor mass development in the flank region of the mice caused a reduction in the Hb level and RBC count. IP administration of BA caused a significant increase in the Hb level (12.6 ± 0.57 g/dl), RBC count (4.33 ± 0.41 million/cmm), and platelet count (218,333 ± 58,380 per cmm) compared to the tumor control group (9.5 ± 0.7 g/dl, 3.4 ± 0.3 million/mm^3, and 123,333 ± 5773 per mm, respectively) on the day of sacrifice ($p < 0.01$). The animals treated with DOX (positive control) showed a low Hb content (6.93 ± 0.7 g/dl) but an enhanced RBC count (4.03 ± 0.05 million/mm^3) and platelet count (226,666 ± 15,275 per cmm). However, the BA-treated group showed a reduction in the WBC count (8533 ± 251 per cmm) ($p < 0.01$) compared to the tumor control group (11,633 ± 300 per cmm). The DOX-treated group also showed a reduction in the WBC count (7200 ± 115 per cmm). These results suggest that IP administration of BA resists the aggravation of the hematological profile associated with the tumor growth. Deterioration of the hematological profile, marked by traits such as anemia, and an increase in WBC levels are often seen in tumors.[37] The observed effects of BA, that is, its ability to elevate the Hb and platelet levels and its ability to suppress the abnormal increase in WBC levels in tumor-bearing mice could thus be seen as indicators of its promising anti-cancer activity against cervical cancer.

Liver injury is a trait exhibited by tumors and the accompanying inflammatory response.[38] Serum biomarkers such as alkaline phosphatase (ALP), glutamic oxalo-acetic transaminase (SGOT), and glutamic-pyruvic transaminase (SGPT) are widely accepted liver function markers to assess the hepatic injury.[39] The BA-treated mice group showed significant reduction in levels of ALP (83 ± 5.2 IU/L), SGOT

https://doi.org/10.1021/acsomega.2c08080
ACS Omega 2023, 8, 10383−10396

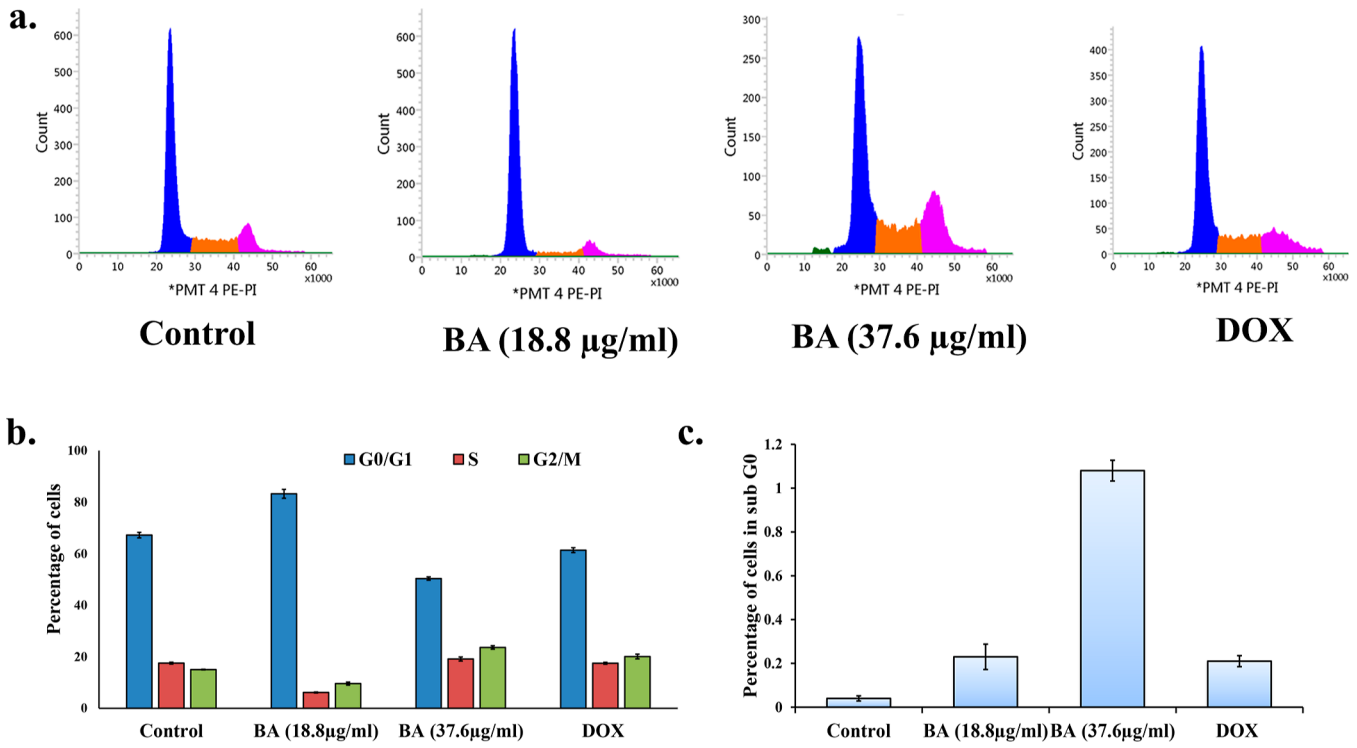

Figure 6. Cell cycle analysis of control and treated (BA and DOX) SiHa cells at 24 h of incubation period. (a) Histogram and (b) graphical representation of G0/G1, S, and G2/M phase cells and (c) percentage of sub G0 cells after treatment for 24 h. Data were expressed as mean ± SD.

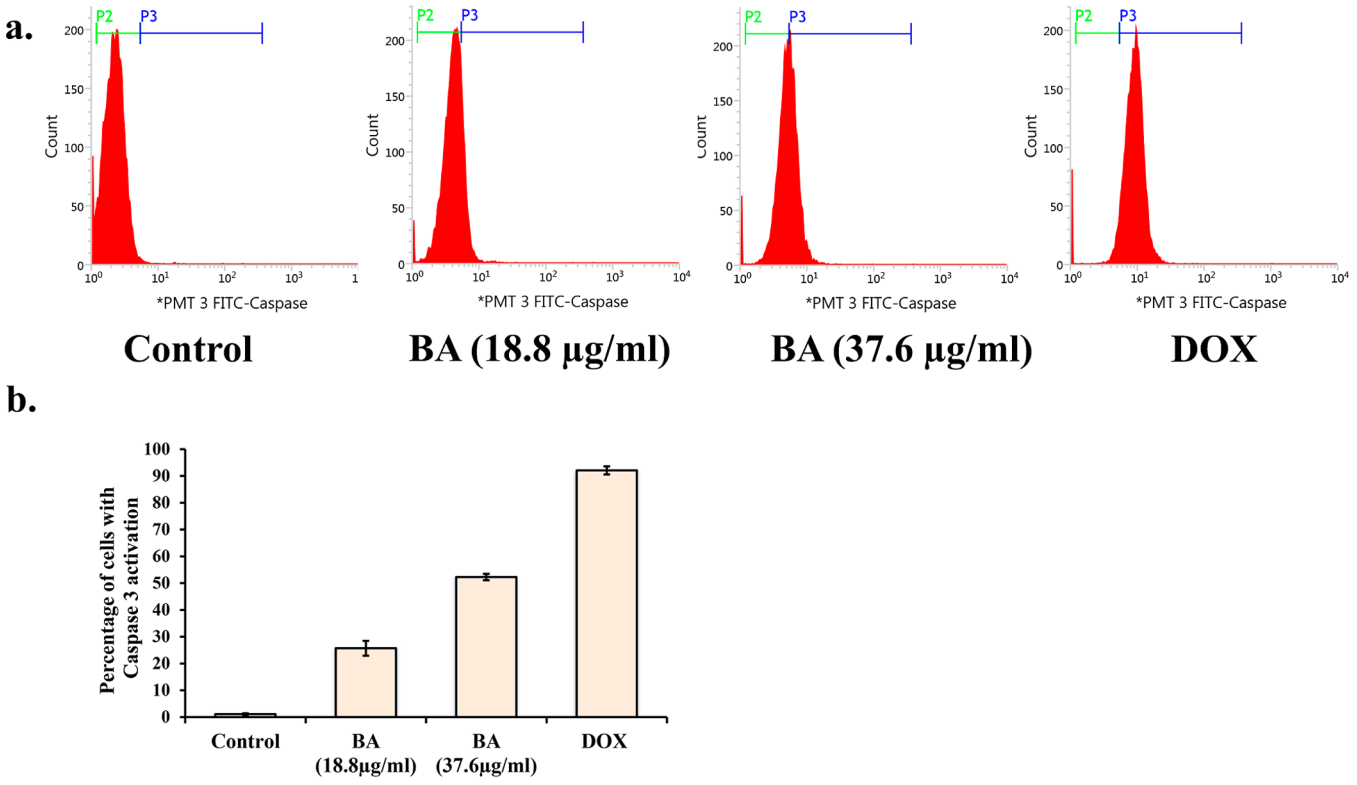

Figure 7. Flow cytometry analysis of activity of caspase 3 on SiHa cell lines after 24 h treatment with BA. (a) Histogram and (b) graphical representation of the percentage of Caspase 3-positive cells. Data were expressed as mean ± SD.

(199.66 ± 12.8 IU/L), and SGPT (69 ± 3 IU/L) compared to the control tumor-bearing group (111.66 ± 7.6, 285.66 ± 2.1, and 143.33 ± 5.7 IU/L, respectively) ($p < 0.01$) (Figure 9). DOX treatment was also found to reduce the levels of these enzymes (106.66 ± 2.8, 85.6 ± 1.1, and 28.6 ± 0.5 IU/L, respectively) indicating that BA treatment resists hepatocellular injury in cervical cancer. Thus, altogether, the *in vivo* studies have proved that BA could be ranked as a potent anti-

https://doi.org/10.1021/acsomega.2c08080
ACS Omega 2023, 8, 10383−10396

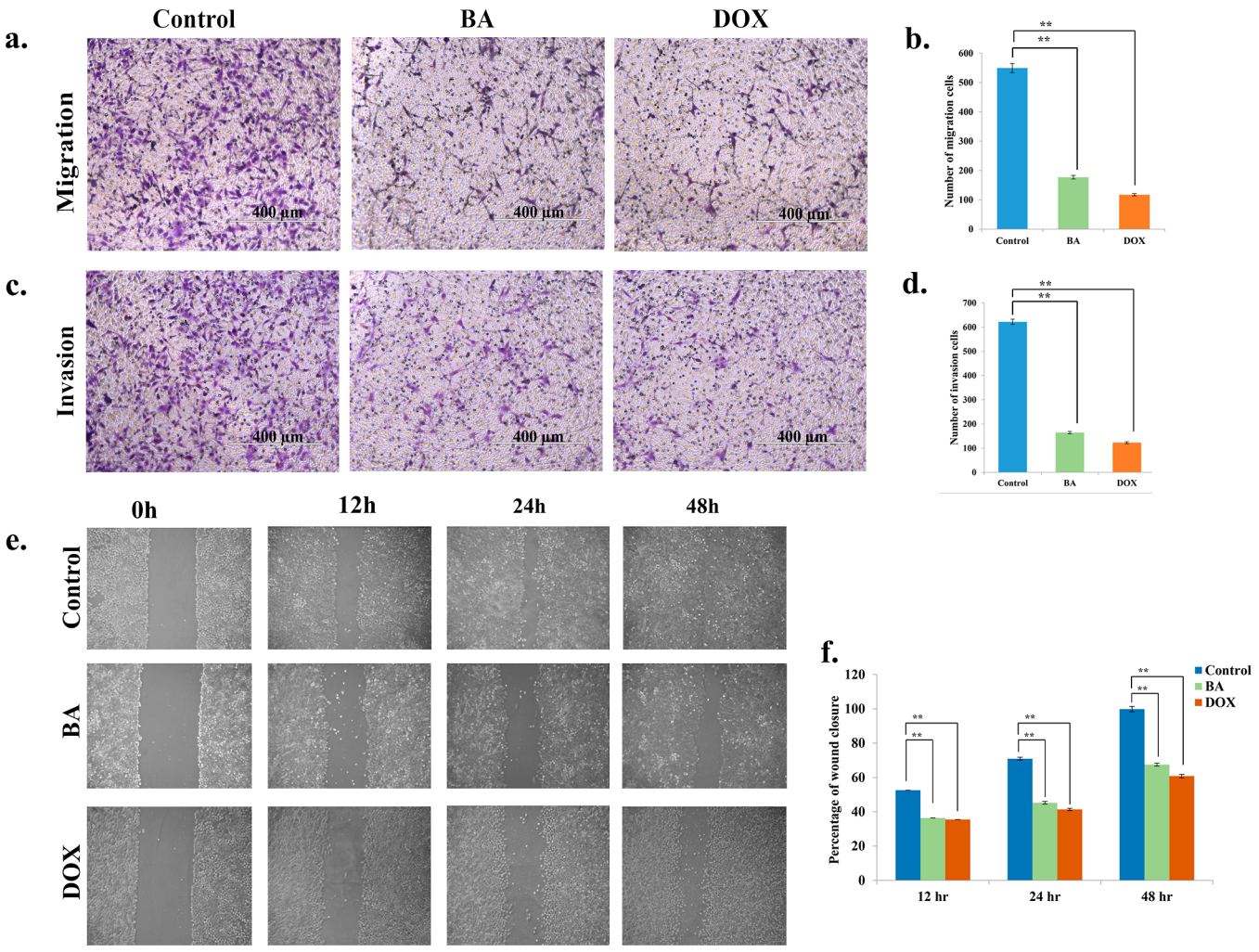

Figure 8. Effects of BA on the cell migration (a,b), invasion (c,d), and wound healing (e,f) of SiHa cells and their graphical quantification. The assays were carried out in triplicates, and the data were expressed as mean ± standard error of mean. Statistical significance is at $^{**}p < 0.001$ with respect to the control.

cancer candidate imposing maximum cytotoxicity on tumor mass without intruding on host health. Clinical trials can be initiated with this molecule for HPV-associated cancers.

METHODS

Plant Collection, Identification, and Extraction. The plant materials were collected from the southernmost district of coastal Kerala and were identified by taxonomists in J N T B G R I, and a voucher specimen (no. 95943) was deposited in the institute herbarium. The plant roots were cleaned in distilled water, shade-dried at room temperature, and pulverized. The root powder (3 kg) was subjected for sequential extraction in the Soxhlet apparatus using the solvents such as PE (BP 38−60 °C), chloroform (BP 61.2 °C), EA (BP 77 °C), and methanol (BP 64.7 °C). The extracts obtained were concentrated using a Heidolph rotary evaporator (Superfit Continental Pvt. Ltd Mumbai, India). The yield of the extracts was 12, 13, 20, and 22 g, respectively. The extract was re-suspended in dimethyl sulfoxide (DMSO) and used for *in vitro* studies.

Cell Lines and Culture Conditions. Nine tumor cell lines representing myelogenous leukemia (K562), lung adenocarcinoma (A549), malignant melanoma (A375), colorectal carcinoma (HCT116), hepatocellular carcinoma (HepG2), ER^+, PR^+, $HER2^-$breast cancer (MCF7), triple-negative breast cancer (MDA-MB-231), HPV-negative cervical cancer (C33A), and HPV-positive cervical cancer (SiHa) were procured from the National Centre for Cell Science (NCCS, Pune). Cells were cultured in Dulbecco's modified Eagle's medium (DMEM) (Gibco, Life technologies, USA) supplemented with 10% fetal bovine serum (FBS) and penicillin−streptomycin−amphotericin solution (MP Biomedicals, Irvine, CA, USA) in a humidified atmosphere of 5% CO_2 at 37 °C. Lymphocytes were obtained from a healthy non-smoking donor.

***In Vitro* Assay for Cytotoxicity Activity (MTT Assay).** MTT (3-(4,5-dimethylthiazolyl-2)-2, 5-diphenyltetrazolium bromide) assay was performed using the different extracts on the above mentioned nine cell lines. Briefly, the cells (5×10^3 cells) were cultured in 96-well plates and incubated overnight (at 37 °C and 5% CO_2) with DMEM medium (0.1 mL) supplemented with FBS and antibiotics. After reaching the confluent phase, the medium was removed and replaced with fresh medium (0.1 mL) and incubated with escalating concentrations of the extracts (100, 200, 400, and 800 µg/mL) and incubated (at 37 °C and 5% CO_2) for 48 h. Assay was performed at 24 and 48 h. MTT (1%) was added 4 h before the termination of the incubation period to all the wells. After

https://doi.org/10.1021/acsomega.2c08080
ACS Omega 2023, 8, 10383−10396

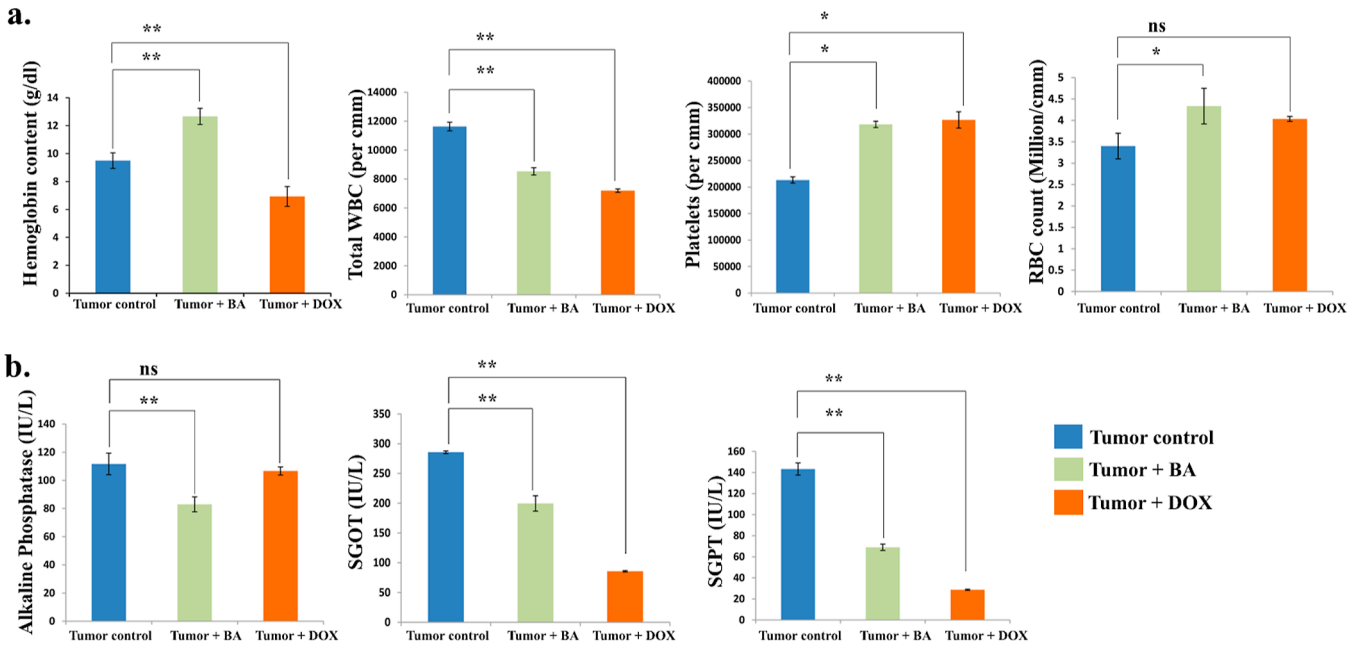

Figure 9. Effect of BA on (a) hematological parameters, namely, Hb, WBC, platelet, and RBC (dl—deciliter and cmm—cubic millimeter) and (b) serum biochemical parameters, namely, ALP, SGOT, and SGPT (IU—international units).

the incubation period, the cells were lysed by adding DMSO/isopropanol (1:1) (0.1 mL) and read at 570 nm with an Epoch microplate spectrophotometer (BioTek, USA). All the experiments were performed in triplicates. The half maximal inhibitory concentration (IC_{50} value) was calculated using the formula

$$\text{percentage inhibition} = 100 - \left\{\left[\frac{(\text{control}_{\text{Abs}} - \text{sample}_{\text{Abs}})}{\text{control}_{\text{Abs}}}\right] \times 100\right\}$$

Lymphocyte Proliferation Assay. Lymphocytes separated from a non-smoking healthy volunteer were used as described previously[10,40] after obtaining approval from human ethics committee of Regional Cancer Centre, Thiruvananthapuram (IRB/08-2014/04). Briefly, blood (3 mL) was collected in heparinized tubes, mixed with phosphate-buffered saline (3 mL), and layered over Ficoll hypaque solution (2 mL). The lymphocytes were separated by centrifugation (2500 rpm for 10 min) and transferred to fresh tubes and washed with phosphate-buffered saline (pH 7.4). The lymphocytes (1×10^4 cells) were seeded in 96-well plates containing DMEM (supplemented with 10% FBS) and incubated with the mitogen phytohemagglutinin (PHA) (0.02 mL, 5 mg/mL) along with escalating concentrations (100, 200, 400, and 800 μg/mL) of the root extract followed by incubation at 37 °C and 5% CO_2 for 72 h. All the experiments were performed in triplicates. After the incubation period, the cells were treated with MTT (1%, 10 mg/mL) and lysed using DMSO/isopropanol as described above, and the absorbance at 570 nm was read and percentage cell viability was calculated.

$$\text{Percentage cell viability} = \left[\frac{(\text{control}_{\text{Abs}} - \text{test}_{\text{Abs}})}{\text{control}_{\text{Abs}}}\right] \times 100$$

Phytochemical Screening and Purification of the Root Extract. Bioassay-guided fractionation and isolation of phytochemicals from *C. infortunatum*-EA were carried out. The extract was chromatographed using a conventional silica gel (100−200 mesh) column eluted in increasing polarities using gradient mixtures of hexane and EA. Nearest fractions with the same R_f values were identified with the help of thin-layer chromatography (TLC) and combined together to form different fraction pools. Separation and purifications of compounds from the respective fraction pools were carried out by repeated column chromatography with silica as the stationary phase and the gradient of hexane and EA as the mobile phase.[41]

The EA extract of root was chromatographed using the silica gel column and eluted with gradient mixtures of hexane and EA in increasing polarities to give six fraction pools (Fr. 1−Fr. 6). Elution started with 100% hexane, and the polarity of the eluting solvent was increased by increasing the amount of EA in hexane−EA mixtures. Final elution was carried out with the 20% methanol−EA system. Different fractions of approximately 500 mL volume were collected in conical flasks. A total of 76 fractions were collected. TLC of each fraction was checked, and those fractions whose TLC profile was alike were pooled together to obtain six different fraction pools. Each of these pooled fractions was concentrated by removing the solvent under reduced pressure. After removing the solvent from fractions, they were subjected to further purification and isolation by column chromatography.

Dual AO/EB Fluorescent Staining and Hoechst 33528 Staining. Acridine orange/ethidium bromide dual staining was performed to study the apoptosis-associated changes in the cell membranes as described previously.[42] SiHa cells (1×10^6 cells) were seeded in six-well plates along with DMEM supplemented with FBS (10%) and incubated overnight at 37 °C and 5% CO_2. After attaining 80% confluency, the cells were separately treated with BA (37.6 μg/mL) and the positive control, DOX (1 μg/mL), and incubated for 24 h. Acridine orange and ethidium bromide staining solution [1:1 w/w in phosphate-buffered saline (PBS)] were added and then

https://doi.org/10.1021/acsomega.2c08080
ACS Omega 2023, 8, 10383−10396

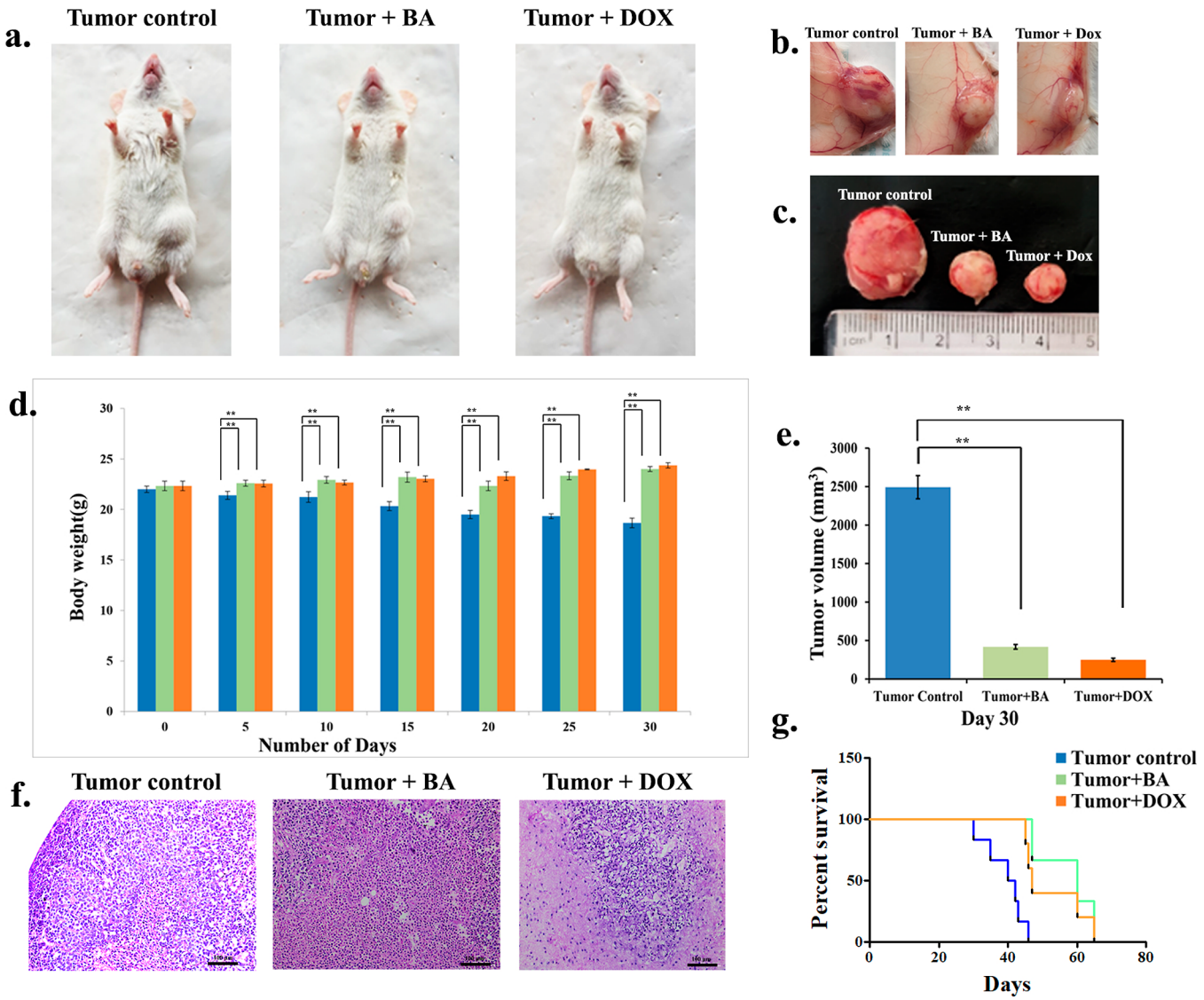

Figure 10. (a) Representative images of NOD/SCID mice from each group and (b&c) images of resected tumor mass on the euthanized day. (d) Effect of BA and DOX on body weight of mice bearing SiHa tumor, (e) tumor volume, and (f) histopathological changes in tumor mass sections in H&E staining and (g) Kaplan Meier survival plots of tumor control, BA-treated, and DOX (positive control)-treated mice.

observed under 40× magnifications in an inverted fluorescent microscope (EVOS FLC, Invitrogen, USA) using a UV filter.

Hoechst 33528 (Life technologies, Eugine, OR, USA) staining was performed similarly in cells treated as mentioned above. The stained cells were observed under 40× magnification of an inverted fluorescent microscope using an FITC filter (EVOS FLC, Invitrogen, USA).[43]

Annexin V—PI Analysis. Apoptotic potential of BA against SiHa cell lines was assessed by the annexin V apoptosis detection kit (BD Pharmingen, cat: no. 556547, San Diego, USA) according to the manufacturer's protocol. Briefly, SiHa cells were seeded in six-well plates at a density of 1×10^6 cells/well and incubated at 37 °C and 5% CO_2. After attaining the required confluency, the cells were treated with different concentrations of BA (18.8 and 37.6 μg/mL) and DOX (positive control) and incubated for 24 h. The cells were then trypsinized and rinsed twice with PBS and then suspended in 500 μL of 1× binding buffer followed by staining with 5 μL of annexin V FITC and 5 μL of PI at room temperature for 15 min in the dark. Cells were resuspended with 400 μL of 1× binding buffer and analyzed by flow cytometry using 488 nm excitation and emission collected at 530/40 for FITC and 585/29 for PI (FACS Jazz, BD, USA).[44]

Cell Cycle Analysis. SiHa cells (1×10^6) were seeded in six-wellwell plates. After 24 h treatment with IC_{50} concentration of BA and DOX, cells were washed twice with ice cold PBS, fixed in pre-cooled 70% ethanol at 4 °C for 2 h, and then centrifuged at 2000 rpm in a refrigerated centrifuge for 5 min. Traces of ethanol were completely removed with 1× PBS and stained with 0.02 mg/mL propidium iodide (Sigma-Aldrich, USA) and 0.1 mg/mL ribonuclease A (Sigma-Aldrich, USA) re-suspended in 200 μL of PBS. The tubes were gently vortexed and kept in the dark at 37 °C for 15 min. Finally, the samples were made up to 500 μL with PBS and measured flow cytometrically using the 488/585 ± 29 filter (FACS Jazz, BD, USA).[45]

Caspase-3 Assay. The FITC active caspase-3 apoptosis kit (BD Pharmingen, cat: no. 550480, San Diego, USA) was used as per the guidelines of the manufacturer. Briefly, control, BA-, and DOX (positive control)-treated (24 h) cells (1×10^6

https://doi.org/10.1021/acsomega.2c08080
ACS Omega 2023, 8, 10383−10396

cells/0.5 mL) were stained for caspase activity and analyzed flow cytometrically using 488 nm excitation and emission collected at 530/40 for FITC (FACS Jazz, BD, US).

Tumor Invasion and Migration Analysis. To evaluate the anti-invasion and anti-migration potential of BA in SiHa cells was performed using transwell invasion, transwell migration and wound healing assay. Transwell inserts (8 μm pore size polycarbonate filters) were coated with 100 μL of solidified MaxGel (Matrigel) ECM (E0282 Sigma-Aldrich, USA; 1:100 dilutions in DMEM only) and incubated for 4 h at 37 °C and under 5% CO_2 condition.[46,47] SiHa cells were seeded (1×10^6 cells/mL) onto each Transwell chambers in serum-free medium with BA (37.6 μg/mL) and DOX (positive control). DMEM medium supplemented with 10% FBS was added onto the lower chamber of transwell insert which act as the chemo-attractant. After 24 h of incubation, the inserts were removed and the inner sides of the inserts were swabbed to remove the non-invaded cells. Cells were fixed using ice cold methanol for 10 min and stained using 1% crystal violet (Himedia GRM961, USA) followed by tap water washing. Membranes were air-dried, and images of invaded cells were captured in an inverted microscope (EVOS FLC, Invitrogen, USA). Along with this, the migration assay was carried out using the same protocol avoiding the MaxGel (Matrigel) ECM-coating step.

Wound Healing Assay (Scratch Assay). Cell to cell interaction along with cell migration and proliferation potential was evaluated by wound healing assay (scratch assay).[48] SiHa (1×10^6) cells were grown in 10% FBS-supplemented DMEM medium on six-well cell culture plates. After the cells attained confluence, a straight wound or scratch was created on a cell monolayer using a sterile 100 μL micropipette tip. BA was added to the cells and kept at 37 °C in a 5% CO_2 incubator. The cells were viewed at 10× objective in a phase-contrast inverted microscope (Olympus BX51, Singapore), and images were captured using a CCD color camera (Nikon, Japan) at intermittent time points (0, 12, 24, and 48 h) until the scratch introduced was completely closed. The scratched area was quantified using Image J software (version 1.5i). The cell migration rate was calculated using the formula

$$\%\ \text{of wound closure} = \frac{(\text{area of the initial wound at time } t_0 - \text{area of the wound at time } t_1)}{\text{area of the initial wound at time } t_0} \times 100$$

A graph was plotted by taking BA on the *X*-axis and the percentage of wound closure on the *Y*-axis.

***In Vivo* Studies.** Female NOD/SCID mice (5−6 weeks old; 20−23 g body weight) obtained from Rajiv Gandhi Centre for Biotechnology, Kerala, India, were maintained in individually ventilated cages under controlled air conditions at a temperature of 20−25 °C and 50−65% humidity in the animal house facility of Regional Cancer Centre, Trivandrum, Kerala, India. The animals were fed with standard high-protein pellet diet (Amrut feeds) and water *ad libitum*. All animal experiment protocols were approved by the Institutional Animal Ethics Committee (IAEC), Regional Cancer Centre (IAEC/RCC no. 2/20), according to the rules laid down by CPCSEA (Committee for the Purpose of Control and Supervision of Experiments on Animals).

Tumor Xenograft in NOD/SCID Mice and Drug Administration. SiHa cells (1×10^6) in PBS (0.1 mL) were injected subcutaneously into the left lower flank of each NOD/SCID mouse to obtain cervical cancer xenografts, and the tumor growth was monitored. When the tumor volume reached about 50 mm^3, the mice were grouped into group 1—tumor control, group 2—tumor + BA, and group 3—tumor + doxorubicin (DOX), each group containing 12 animals. Mice in group 2, which were intraperitoneally injected with BA at 10 mg/kg body weight per day served as the experimental drug-treated group. Mice in group 3, which were treated with DOX (10 mg/kg body weight for 10 consecutive days), served as the group treated with standard drug. Mice belonging to group 1 (the tumor-bearing control group) were injected with 100 μL of PBS (pH-7.4) daily for 10 consecutive days.[49−51] Six animals from each group were sacrificed by cervical dislocation on day 30. The remaining mice were monitored for survival analysis.

Tumor Mass Study, Hematological—Biochemical and Histopathological Examinations. At the end of the experiment, blood samples were collected for assessing hematological and biochemical parameters. The tumor xenografts were removed, and the tumor volume was calculated using the formula $4/3\pi\ r_1^2 r_2$, where r_1 and r_2 are the radii of the tumors at two different planes. The extent of neovascularization around the tumors was visualized in the inner peritoneal lining of the experimental animals at the time of resection of tumor xenografts. Excised tumor xenografts were weighed and fixed in 10% formalin and embedded in paraffin blocks, and 4 μm thin sections of the tissue samples were obtained on a rotary microtome (Leica, JUNG RM 2025, Germany) and then de-paraffinized with xylene, hydrated, and stained with haematoxylin and eosin (H&E).[52] All stained tissue sections were examined under a light microscope (Leica 20× magnification) for histopathological changes.

Statistical Analysis. All the experiments were performed in triplicates, and values were expressed as mean ± standard deviation (SD). Statistical analysis was performed using one-way ANOVA followed by Dunnett's post hoc test using Instat version 3.06 (GraphPad Software, USA). A *p*-value of less than 0.05 was considered to be statistically significant.

CONCLUSIONS

Despite the rapid reduction in the incidence of cervical cancer following Pap smear screening, HPV DNA test, and vaccination in the developed world, cervical cancer continues to take extraordinary toll on the lives of women in India and other developing countries. Also, an increased recurrence rate for cervical cancer has been reported in recent years, and treatment of recurrent cervical cancer remains challenging. Therefore, there is an increasing demand for newer drugs for the effective management of this disease. The use of *C. infortunatum* in cancer therapy has been already in practice by several traditional healers. Swami Nirmalananda Giri has patented the process for the preparation of the plant extract and claimed it for curing cervical cancer (US 2014/0134731 A1), and the active compound has been reported as a glycoprotein, which formed the rationale for the current study. *C. infortunatum* root decoction has been prescribed as a post-partum care, which has been argued to offer protection against cervical cancer. However, there are no further scientific studies to substantiate the same. The present study had found that BA is the active fraction responsible for the cytotoxic activity of the *C. infortunatum* root extract. The putative role of this molecule in triggering apoptosis, inhibiting cell migration, and neo-angiogenesis has been well documented. This is the first report on the antineoplastic effect of BA on the xenograft developed

https://doi.org/10.1021/acsomega.2c08080
ACS Omega 2023, 8, 10383−10396

from HPV-positive SiHa cells, suggesting its potential role to clear HPV infection, even though the compound is not a novel one. Also, it did not cause any significant adverse side effect similar to the current chemotherapeutic drugs. All these observations confirm the prospective of this molecule for moving to a clinical trial and developing as a potential commercial drug for HPV-associated malignancies, which in our knowledge is the first report. Local application of the root extract of *C. infortunatum* may be tried in the preselected cervical intraepithelial lesions and other preneoplastic lesions associated with HPV infection so that many of the cancers can be prevented.

■ ASSOCIATED CONTENT

Supporting Information

The Supporting Information is available free of charge at https://pubs.acs.org/doi/10.1021/acsomega.2c08080.

Materials and methods used for the isolation of compounds; extraction and isolation diagram; and ^{1}H and ^{13}C NMR spectra of the isolated compounds (PDF)

■ AUTHOR INFORMATION

Corresponding Authors

Kokkuvayil Vasu Radhakrishnan − *Chemical Sciences and Technology Division, CSIR-National Institute for Interdisciplinary Science and Technology, Trivandrum, Kerala 695 019, India;* orcid.org/0000-0001-8909-3175; Email: radhu2005@gmail.com

Kunjuraman Sujathan − *Division of Cancer Research, Regional Cancer Centre, Trivandrum 695 011, India;* Phone: 91-0471-2522282, 91-0471-2447454; Email: ksujathan@gmail.com

Authors

Balakrishnan Syamala Akhil − *Manipal Academy of Higher Education, Manipal, Karnataka 576104, India; Division of Cancer Research, Regional Cancer Centre, Trivandrum 695 011, India;* orcid.org/0000-0002-5736-1291

Rajimol Puthenpurackal Ravi − *Chemical Sciences and Technology Division, CSIR-National Institute for Interdisciplinary Science and Technology, Trivandrum, Kerala 695 019, India; Academy of Scientific and Innovative Research (AcSIR), Ghaziabad 201 002, India;* orcid.org/0000-0002-7046-3428

Asha Lekshmi − *Division of Cancer Research, Regional Cancer Centre, Trivandrum 695 011, India*

Prathapan Abeesh − *Division of Cancer Research, Regional Cancer Centre, Trivandrum 695 011, India*

Chandrasekharan Guruvayoorappan − *Division of Cancer Research, Regional Cancer Centre, Trivandrum 695 011, India;* orcid.org/0000-0001-6356-2893

Complete contact information is available at: https://pubs.acs.org/10.1021/acsomega.2c08080

Author Contributions

$^{\perp}$B.S.A. and R.P.R. contributed equally to this work

Notes

The authors declare no competing financial interest.

■ ACKNOWLEDGMENTS

The authors wish to acknowledge DBT, Govt. of India (no. BT/PR/6483/MED/30/862/2012; Dated: 06/02/2015), for providing research funding to Dr. Kunjuraman Sujathan. The support from Biji M, SRF, CSTD, CSIR-NIIST, Trivandrum, for NMR structural analysis and Aswathy M, SRF, CSTD, CSIR-NIIST, Trivandrum, for reviewing the manuscript has been acknowledged. Dr. Biba Vikas and Dr. Unnikrishnan B. S. have been acknowledged for their support in executing the experiments.

■ ABBREVIATIONS

BA, betulinic acid; HPV, human papilloma virus; PE, petroleum ether extract; CL, chloroform extract; EA, ethyl acetate extract; ME, methanol extract; DOX, doxorubicin

■ REFERENCES

(1) Singh, S.; Sharma, B.; Kanwar, S. S.; Kumar, A. Lead phytochemicals for anticancer drug development. *Front. Plant Sci.* **2016**, *7*, 1667.

(2) Gera, N. B.; Darshani, P. P. Chemical composition of a volatile fraction from the leaves of Clerodendrum infortunatum L. *Nat. Prod. Res.* **2022**, *36*, 853−856.

(3) Swargiary, A.; Brahma, K.; Boro, T.; Daimari, M.; Roy, M. K. Study of phytochemical content, antioxidant and larvicidal property of different solvent extracts of Clerodendrum infortunatum and Citrus grandis. *Indian J. Tradit. Knowl.* **2021**, *20*, 329−334.

(4) Nandi, S.; Lyndem, L. M. Clerodendrum viscosum: traditional uses, pharmacological activities and phytochemical constituents. *Nat. Prod. Res.* **2016**, *30*, 497−506.

(5) Helen, R.; Jayesh, K.; Syama, S.; Latha, M. Secondary Metabolites from Clerodendrum Infortunatum L.: Their Bioactivities and Health Benefits. In *Health Benefits of Secondary Phytocompounds from Plant and Marine Sources*, 1st ed.; Apple Academic Press: London, 2021; pp 39−60.

(6) Uddin, M.; Russo, D.; Haque, M.; Çiçek, S. S.; Sönnichsen, F. D.; Milella, L.; Zidorn, C. Bioactive Abietane-Type Diterpenoid Glycosides from Leaves of Clerodendrum infortunatum (Lamiaceae). *Molecules* **2021**, *26*, 4121.

(7) Sun, C.; Nirmalananda, S.; Jenkins, C.; Debnath, S.; Balambika, R.; Fata, J.; Raja, K. First ayurvedic approach towards green drugs: anti cervical cancer-cell properties of Clerodendrum viscosum root extract. *Anti-Cancer Agents Med. Chem.* **2013**, *13*, 1469−1476.

(8) Das, B.; Pal, D.; Haldar, A. A review on biological activities and medicinal properties of Clerodendrum infortunatum Linn. *Int. J. Pharm. Pharmaceut. Sci.* **2014**, *6*, 41−43.

(9) Haris, M.; Mahmood, R.; Rahman, H.; Rahman, N. In vitro cytotoxic activity of Clerodendrum infortunatum L. Against T47D, PC-3, A549 and HCT-116 human cancer cell lines and its phytochemical screening. *Int. J. Pharm. Pharmaceut. Sci.* **2016**, *8*, 439−444.

(10) Varalakshmi, K.; Sangeetha, C.; Samee, U.; Irum, G.; Lakshmi, H.; Prachi, S. In vitro safety assessment of the effect of five medicinal plants on human peripheral lymphocytes. *Trop. J. Pharmaceut. Res.* **2011**, *10*, 33−40.

(11) Nweze, C.; Ibrahim, H.; Ndukwe, G. Beta-sitosterol with antimicrobial property from the stem bark of pomegranate (Punica granatum Linn). *J. Appl. Sci. Environ. Manag.* **2019**, *23*, 1045−1049.

(12) Khan, M. E.; Bala, L. M.; Maliki, M. Phytochemical analyses of Terminalia schimperiana (Combretaceae) root bark extract to isolate stigmasterol. *Int. J. Adv. Chem.* **2019**, *2*, 327−334.

(13) Joshua, J.; Oyewale, A.; Ibrahim, H. Isolation, Characterization and Antimicrobial Screening of Betulinic Acid from the Stem Extract of Fadogia erythrophloea. *J. Chem. Soc. Niger.* **2020**, *45*, 620−629.

(14) Phan, M. G.; Do, T. V. H.; Nguyen, Q. B. Methylated Flavonols from Amomum koenigii JF Gmel. and Their Antimicrobial and Antioxidant Activities. *Biochem. Res. Int.* **2020**, *2020*, 1−6.

(15) Seebacher, W.; Simic, N.; Weis, R.; Saf, R.; Kunert, O. Complete assignments of 1H and 13C NMR resonances of oleanolic

https://doi.org/10.1021/acsomega.2c08080
ACS Omega 2023, 8, 10383−10396

acid, 18α-oleanolic acid, ursolic acid and their 11-oxo derivatives. *Magn. Reson. Chem.* **2003**, *41*, 636−638.
(16) Malan, E.; Roux, D. G. Flavonoids from Distemonanthus benthamianus Baillon. Methoxylated flavones and inter-relationships of benthamianin, a [2] benzopyrano [4, 3-b][1] benzopyran. *J. Chem. Soc., Perkin Trans. 1* **1979**, 2696−2703.
(17) Sambandam, B.; Thiyagarajan, D.; Ayyaswamy, A.; Raman, P. Extraction and isolation of flavonoid quercetin from the leaves of Trigonella foenum-graecum and their anti-oxidant activity. *J. Pharm. Pharmaceut. Sci.* **2016**, *8*, 120−124.
(18) Bringmann, G.; Saeb, W.; Assi, L. A.; François, G.; Sankara Narayanan, A. S.; Peters, K.; Peters, E.-M. Betulinic acid: isolation from Triphyophyllum peltatum and Ancistrocladus heyneanus, antimalarial activity, and crystal structure of the benzyl ester. *Planta Med.* **1997**, *63*, 255−257.
(19) Chandramu, C.; Manohar, R. D.; Krupadanam, D. G.; Dashavantha, R. V. Isolation, characterization and biological activity of betulinic acid and ursolic acid from Vitex negundo L. *Phytother Res.* **2003**, *17*, 129−134.
(20) Csuk, R. Betulinic acid and its derivatives: A patent review (2008−2013). *Expert Opin. Ther. Pat.* **2014**, *24*, 913−923.
(21) Kessler, J. H.; Mullauer, F. B.; de Roo, G. M.; Medema, J. P. Broad in vitro efficacy of plant-derived betulinic acid against cell lines derived from the most prevalent human cancer types. *Cancer Lett.* **2007**, *251*, 132−145.
(22) Park, C.; Jeong, J.-W.; Han, M. H.; Lee, H.; Kim, G.-Y.; Jin, S.; Park, J.-H.; Kwon, H. J.; Kim, B. W.; Choi, Y. H. The anti-cancer effect of betulinic acid in u937 human leukemia cells is mediated through ROS-dependent cell cycle arrest and apoptosis. *Anim. Cell Syst.* **2021**, *25*, 119−127.
(23) Dutta, D.; Paul, B.; Mukherjee, B.; Mondal, L.; Sen, S.; Chowdhury, C.; Debnath, M. C. Nanoencapsulated betulinic acid analogue distinctively improves colorectal carcinoma in vitro and in vivo. *Sci. Rep.* **2019**, *9*, 1−20.
(24) Fulda, S. Betulinic acid for cancer treatment and prevention. *Int. J. Mol. Sci.* **2008**, *9*, 1096−1107.
(25) Fulda, S.; Friesen, C.; Los, M.; Scaffidi, C.; Mier, W.; Benedict, M.; Nuñez, G.; Krammer, P. H.; Peter, M. E.; Debatin, K. M. Betulinic acid triggers CD95 (APO-1/Fas)-and p53-independent apoptosis via activation of caspases in neuroectodermal tumors. *Cancer Res.* **1997**, *57*, 4956.
(26) Santos, R. C.; Salvador, J. A.; Cortés, R.; Pachón, G.; Marín, S.; Cascante, M. New betulinic acid derivatives induce potent and selective antiproliferative activity through cell cycle arrest at the S phase and caspase dependent apoptosis in human cancer cells. *Biochimie* **2011**, *93*, 1065−1075.
(27) Xu, Y.; Li, J.; Li, Q.-J.; Feng, Y.-L.; Pan, F. Betulinic acid promotes TRAIL function on liver cancer progression inhibition through p53/Caspase-3 signaling activation. *Biomed. Pharmacother.* **2017**, *88*, 349−358.
(28) Jiang, W.; Li, X.; Dong, S.; Zhou, W. Betulinic acid in the treatment of tumour diseases: Application and research progress. *Biomed. Pharmacother.* **2021**, *142*, 111990.
(29) Ganguly, A.; Das, B.; Roy, A.; Sen, N.; Dasgupta, S. B.; Mukhopadhayay, S.; Majumder, H. Betulinic acid, a catalytic inhibitor of topoisomerase I, inhibits reactive oxygen species−mediated apoptotic topoisomerase I−DNA cleavable complex formation in prostate cancer cells but does not affect the process of cell death. *Cancer Res.* **2007**, *67*, 11848−11858.
(30) Kim, S. Y.; Hwangbo, H.; Kim, M. Y.; Ji, S. Y.; Kim, D. H.; Lee, H.; Kim, G.-Y.; Moon, S.-K.; Leem, S.-H.; Yun, S. J. Betulinic acid restricts human bladder cancer cell proliferation in vitro by inducing caspase-dependent cell death and cell cycle arrest, and decreasing metastatic potential. *Molecules* **2021**, *26*, 1−18.
(31) Sakthive, K.; Kannan, N.; Angeline, A.; Guruvayoorappan, C. Anticancer activity of Acacia nilotica (L.) Wild. Ex. Delile subsp. indica against Dalton's ascitic lymphoma induced solid and ascitic tumor model. *Asian Pac. J. Cancer Prev.* **2012**, *13*, 3989−3995.
(32) Abeesh, P.; Rasmi, R. R.; Guruvayoorappan, C. Edible sword bean extract induces apoptosis in cancer cells in vitro and inhibits ascites and solid tumor development in vivo. *Nutr. Cancer* **2021**, *73*, 1015−1025.
(33) Sudarsanan, D.; Sulekha, D. S.; Chandrasekharan, G. Amomum subulatum induces apoptosis in tumor cells and reduces tumor burden in experimental animals via modulating pro-inflammatory cytokines. *Cancer Invest.* **2021**, *39*, 333−348.
(34) Xia, C.; He, Z.; Liang, S.; Chen, R.; Xu, W.; Yang, J.; Xiao, G.; Jiang, S. Metformin combined with nelfinavir induces SIRT3/mROS-dependent autophagy in human cervical cancer cells and xenograft in nude mice. *Eur. J. Pharmacol.* **2019**, *848*, 62−69.
(35) Makrilia, N.; Lappa, T.; Xyla, V.; Nikolaidis, I.; Syrigos, K. The role of angiogenesis in solid tumours: an overview. *Eur. J. Intern. Med.* **2009**, *20*, 663−671.
(36) Wang, Z.; Dabrosin, C.; Yin, X.; Fuster, M. M.; Arreola, A.; Rathmell, W. K.; Generali, D.; Nagaraju, G. P.; El-Rayes, B.; Ribatti, D.; Chen, Y. C.; Honoki, K.; Fujii, H.; Georgakilas, A. G.; Nowsheen, S.; Amedei, A.; Niccolai, E.; Amin, A.; Ashraf, S. S.; Helferich, B.; Yang, X.; Guha, G.; Bhakta, D.; Ciriolo, M. R.; Aquilano, K.; Chen, S.; Halicka, D.; Mohammed, S. I.; Azmi, A. S.; Bilsland, A.; Keith, W. N.; Jensen, L. D. Broad targeting of angiogenesis for cancer prevention and therapy. *Semin. Cancer Biol.* **2015**, *35*, S224−S243.
(37) Jounblat, Y.; El Hachem, G. J. J. H. T. Anaemia in metastatic solid tumors: a frequent and serious finding. small review of the literature. *J. Hematol. Blood Transfus.* **2017**, *5*, 1073.
(38) Shivaraj, G.; Prakash, D.; Vinayak, H.; Avinash, M.; Sonal, V.; Shruthi, K. A review on laboratory liver function tests. *Pan Afr. Med. J.* **2009**, *3*, 17.
(39) Limdi, J.; Hyde, G. Evaluation of abnormal liver function tests. *Postgrad. Med. J.* **2003**, *79*, 307−312.
(40) Suman, G.; Jamil, K. Application of human lymphocytes for evaluating toxicity of anti-cancer drugs. *Pharmacol* **2006**, *2*, 374−381.
(41) Sarker, S. D.; Nahar, L. An introduction to natural products isolation. *Methods Mol. Biol.* **2012**, *864*, 1−25.
(42) Liu, K.; Liu, P.-c.; Liu, R.; Wu, X. Dual AO/EB staining to detect apoptosis in osteosarcoma cells compared with flow cytometry. *Med. Sci. Mon. Basic Res.* **2015**, *21*, 15−20.
(43) Bhavana, J.; Kalaivani, M.; Sumathy, A. Cytotoxic and pro-apoptotic activities of leaf extract of Croton bonplandianus Baill. against lung cancer cell line A549. *Indian J. Exp. Biol.* **2016**, *54*, 379.
(44) Zhao, J.; Li, R.; Pawlak, A.; Henklewska, M.; Sysak, A.; Wen, L.; Yi, J.-E.; Obmińska-mrukowicz, B. Antitumor activity of betulinic acid and betulin in canine cancer cell lines. *Eur. J. Pharmacol.* **2018**, *32*, 1081−1088.
(45) Pan, Z.; Zhang, X.; Yu, P.; Chen, X.; Lu, P.; Li, M.; Liu, X.; Li, Z.; Wei, F.; Wang, K.; Zheng, Q.; Li, D. Cinobufagin induces cell cycle arrest at the G2/M phase and promotes apoptosis in malignant melanoma cells. *Front. Oncol.* **2019**, *9*, 853.
(46) Li, J.; Khan, M.; Wei, C.; Cheng, J.; Chen, H.; Yang, L.; Ijaz, I.; Fu, J. J. M. Thymoquinone inhibits the migration and invasive characteristics of cervical cancer cells SiHa and CaSki in vitro by targeting epithelial to mesenchymal transition associated transcription factors Twist1 and Zeb1. *Molecules* **2017**, *22*, 2105.
(47) Shi, Y.-H.; Tuokan, T.; Lin, C.; Chang, H. Aquaporin 8 involvement in human cervical cancer SiHa migration via the EGFR-Erk1/2 pathway. *Asian Pac. J. Cancer Prev.* **2014**, *15*, 6391−6395.
(48) Liang, C.-C.; Park, A. Y.; Guan, J.-L. In vitro scratch assay: a convenient and inexpensive method for analysis of cell migration in vitro. *Nat. Protoc.* **2007**, *2*, 329−333.
(49) Wei, W.-F.; Han, L.-F.; Liu, D.; Wu, L.-F.; Chen, X.-J.; Yi, H.-Y.; Wu, X.-G.; Zhong, M.; Yu, Y.-h.; Liang, L. Orthotopic xenograft mouse model of cervical cancer for studying the role of microRNA-21 in promoting lymph node metastasis. *Int. J. Gynecol. Cancer* **2017**, *27*, 1−9.
(50) Sham, E.; Durand, R. E. Repopulation characteristics and cell kinetic parameters resulting from multi-fraction irradiation of xenograft tumors in SCID mice. *Eur. J. Cancer* **1999**, *43*, 617−622.

https://doi.org/10.1021/acsomega.2c08080
ACS Omega 2023, 8, 10383−10396

(51) Cai, H.; Yan, L.; Liu, N.; Xu, M.; Cai, H. IFI16 promotes cervical cancer progression by upregulating PD-L1 in immunomicroenvironment through STING-TBK1-NF-kB pathway. *Biomed. Pharmacother.* **2020**, *123*, 109790.
(52) Cardiff, R. D.; Miller, C. H.; Munn, R. J. Manual hematoxylin and eosin staining of mouse tissue sections. *Cold Spring Harb. Protoc.* **2014**, *2014*, 655.

https://doi.org/10.1021/acsomega.2c08080
ACS Omega 2023, 8, 10383−10396